# INHIBITORY ACTIVITY OF PALMATINE ON MAIN PROTEASE COMPLEX ($M^{pro}$) OF SARS-CoV-2

*V.A. JADHAV*,**#, SUJATA INGLE*, R. AHMED**

*School of Life Sciences, "Swami Ramanand Teerth Marathwada" University, Nanded, 431606 (MS), India, #e-mail: vbiophysics@gmail.com
**Department of Biophysics, "Digambarrao Bindu" College, Bhokar, Nanded District, 431801 (MS), India

*Abstract***.** The pandemic situation caused by SARS-CoV-2 is responsible for the coronavirus infectious disease-19 (COVID-19) around the globe. Recently reported highly modulated enzyme main protease complex ($M^{pro}$) was responsible for coronavirus replication and transcription. This significant function of $M^{pro}$ attracts as potential candidates for drug targets. Naturally, *Tinospora cordifolia* was found effective against cancer, HIV, viral infections and diabetes. One of the most effective alkaloid palmatine present in *T. cordifolia*. In present study, we have investigated potential activity of palmatine against $M^{pro}$. Physico-chemical properties were analyzed by the ProtParam tool; structure prediction and homology modeling were carried out by the SWISS-MODEL server. Significant superimposition structure, equal global model quality estimation (GMQE) and quaternary structure quality estimate (QSQE) values were found for eight highly similar templates. Ramachandran plot (97.67 % favored), local quality estimate ratio (>0.6), and higher qualitative model energy analysis (QMEAN) score (*y*-axis) assessments were performed for structural validation of $M^{pro}$. Further, the SwissDock server was used to perform docking between validated targets $M^{pro}$ with ligand palmatine. The significant $\Delta G$ value –8.281919 kcal·mol$^{-1}$ indicates reliable docking interaction. Comparative docking among palmatine, gingerol and berberine suggests palmatine interacts efficiently with $M^{pro}$. Thus, an attempt was made to find a potent inhibitor, as there is no promising and specific antiviral drug or vaccine available for the prevention and treatment of COVID-19 infections. However, *in vitro* studies are required to validate our predictions. Whereas, toxicological studies reported against palmatine for acute effect (135 mg/kg body weight) on mouse model $LD_{50}$.

*Key words*: Palmatine, SARS-CoV-2, main protease complex, homology modelling, docking.

## INTRODUCTION

Coronaviruses are commonly a group of RNA viruses infecting and causing diseases in birds and mammals, including humans [20]. They belong to subfamily *Orthocoronavirinae* in family *Coronaviridae*, order *Nidovirales* [1]. This group of viruses is a positive-sense ssRNA genome surrounded by a spherical envelope with a genome size ranging from 26 to 32 kb [25, 32].

Received: September 2020;
in final form November 2020.

ROMANIAN J. BIOPHYS., Vol. 31, No. 1, P. 27–40, BUCHAREST, 2021

Recently, a new coronavirus caused a threat around the globe due to severe acute respiratory syndrome coronavirus 2 (SARS-CoV-2) [17]. Humans are mostly affected by respiratory tract infections caused by coronavirus disease in 2019, identified as COVID-19 [17]. Upon infection, mild to death effects have been widely reported in the human population [28]. Currently, there is no promising and specific antiviral drug or vaccine available for the prevention and treatment of infections caused by COVID-19 [28]. Similar varieties of viruses, including SARS and MERs, have divesting effects on human existence in recent decades [6]. Therefore, by considering the present pandemic situation around the globe, it was decided to develop novel and potent strategies.

In the present scenario, the discovery of active components from the plant and their biological function in disease control has led to an active interest in plant products across the globe [26]. Similarly, in modern medicine, many drugs are derived from plant products and their derivatives [26]. A variety of lead compounds was obtained from plant secondary metabolites for the treatment of various diseases [15]. Alkaloids and flavonoids have strong analgesic effects and dietary supplements respectively [26]. The most commonly used secondary metabolite, artemisinin, is a widely used phytomedicine [7].

In the present analysis, an attempt was made to evaluate the antiviral activity of palmatine alkaloid against the COVID-19 main protease complex ($M^{pro}$) of SARS-CoV-2. Alkaloid are found in naturally occurring *Tinospora cordifolia* commonly known as Guduchi [26]. It has been reported for its diverse application in the treatment of various diseases, *i.e.* cancer, HIV, viral infections, neurological diseases, diabetes, etc. [26]. By considering pandemic impact and medical urgency, a computational analysis was performed for the anti-COVID-19 main protease complex of SARS-CoV-2 by potential palmatine alkaloid molecules. The completely characterized COVID-19 main protease complex ($M^{pro}$) is submitted in protein data bank (PDB) [14]. It is a multifunctional and highly modulating enzyme in SARS-CoV-2 replication and transcription [14]. Therefore, the identified COVID-19 main protease complex is attractive as a potential drug target.

## MATERIALS AND METHODS

### INHIBITOR PREPARATION

PubChem [40] database contains validated fulfilled chemical informational data [16]. The plant metabolite palmatine is alkaloid and an organic heterotetracyclic compound [25, 35]. The palmatine was completely characterized and structured with PubChem CID: 19009 [25, 35]. Toxicological studies indicate suitable inhibitor for further analysis [26, 36]. Palmatine as well as gingerol and berberine structure was retrieved from PubChem database.

## PHYSICO-CHEMICAL ANALYSIS

ProtParam [38] tool was used to analyze physical and chemical parameters for a given protein or user-provided protein sequence present in Swiss-Prot or TrEMBL [8]. Then, the FASTA format protein sequence of SARS-CoV-2 $M^{pro}$ was provided in one-letter code for computing parameters.

## $M^{PRO}$ PREPARATION

The crystal structure of SARS-CoV-2 main protease (PDB code: 6LU7) was retrieved from PDB [3, 37]. PDB structure was downloaded for homology modeling and molecular docking analysis with .pdb file format. FASTA format sequences were retrieved from PDB [23].

## HOMOLOGY MODELING

SWISS-MODEL [39] is a protein structure homology modeling server, which facilitates modeling service to life research [17, 31]. FASTA format sequence was submitted to SWISS-MODEL workspace on June 9, 2020 for homology modeling of protein $M^{pro}$. For template search SWISS-MODEL template library was searched against BLAST and HHBlits (SMTL, last update: 2020-06-03, last included PDB release: 2020-05-29) [4]. Features of template-target alignment determine identification and quality of the template for selection. Then, best quality templates were considered for building model [4].

## MODEL BUILDING

ProMod3 predicts model on the target-template alignment [12]. The highly conserved coordinates between the target and the template are taken from the template to the model [12]. Rebuilding of insertions and deletions are remodeled using a fragment library [12]. Finally, the force field method was applied to satisfy the geometry of the predicted model [12]. The global and per-residue model quality has been evaluated using the QMEAN scoring function [29].

## LIGAND MODELLING

Template-ligand structure was validated after satisfying the following criteria by ligand with the model: (a) biological significance and annotation in the template library, (b) proximity, (c) matching, and (d) conserved bonding between the target and template [31]. However, ligands fail to satisfy the criteria and are not included in the model [31].

### OLIGOMERIC STATE CONSERVATION

To model the oligomeric target sequence, the annotated quaternary structure of the template was used [2]. QSQE was determined by supervised machine learning algorithm on the basis of interface conservation, structural clustering and other template aspects [2]. Higher numbers QSQE score is directly proportional to reliability of model [2]. This is synergetic to the global model quality estimate (GMQE) score for predicting the correctness of the resultant model at the tertiary structural level [2].

### MOLECULAR DOCKING

SwissDock [41] is an EADock DSS-based docking service available on the ExPASy web server. It was used to predict protein-ligand docking [10, 11]. The molecular interaction that may occur between a target protein and a small molecule was evaluated [10, 11]. Its algorithm consists of the following steps. Initially, various binding modes are created in the box, *i.e.*, the binding mode. Further, local docking or vicinity of all target cavities, viz. blind docking. Simultaneously, their Charmm [43] energies are estimated. Furthermore, clusters computed by SwissDock were downloaded for further visualization and analysis [11].

## RESULTS

### PHYSIO-CHEMICAL PROPERTIES

The analysis of viral main protease protein using the ProtParam tool provides valuable information about proteins, including the number of amino acids, molecular weight, and theoretical pI (Table 1). The total number of amino acids in protein is 306, while leucine (29 – 9.5 %) is the most frequently occurring amino acids, and the least frequently occurring is Pyl (O) and Sec (U) 0 (0.0 %). The molecular weight was 33796.64 Da (Table 1). The theoretical pI of the protein was 5.95 (Table 1). The total numbers of negatively and positively charged residues are 26 and 22, respectively. The molecular formula is described based on the atomic combination of carbon, hydrogen, nitrogen and oxygen found in protein (Table 1). The extinction coefficient at 280 nm was 33640 $M^{-1} \cdot cm^{-1}$, and an absorption (Abs 0.1 % = 1 g/L) of 0.995 g/L was observed (Table 1). The instability index is inversely proportional to the stability of proteins, with 27.65 observed. The estimated half-life of protein was observed to be 1.9 hours (Table 1).

*Table 1*

Computational analysis of physico-chemical parameters of COVID-19 main protease of SARS-CoV-2 predicted using ProtParam

| Sr. No. | Parameters | COVID-19 main protease complex |
|---|---|---|
| 1 | Theoretical pI | 5.95 |
| 2 | Molecular formula | $C_{1499}H_{2318}N_{402}O_{445}S_{22}$ |
| 3 | Total number of atoms | 4686 |
| 4 | Molecular weight (Da) | 33796.64 |
| 5 | Number of amino acids | 306 |
| 6 | Higher No. of amino acid composition | Leu (L) 29 (9.5 %) |
| 7 | Extinction coefficients ($M^{-1}\cdot cm^{-1}$) at 280 nm in water | 33640 |
| 8 | Abs 0.1 % (= 1 g/L) | 0.995 |

## PROTEIN HOMOLOGY MODELLING

This protein COVID-19 main protease is already predicted and submitted in PDB with PDB Id: 6LU7 [14]. For further validation, homology modeling with SWISS-MODEL was performed. The SWISS-MODEL template library (SMTL version 2020-06-03, PDB release 2020-05-29) was searched with BLAST [4] and HHBlits [22] for identical structures matching with the target sequence.

## MODEL BUILDING

The results for the homology modeling project "COVID-19 main protease complex ($M^{pro}$)" submitted to SWISS-MODEL workspace on June 9, 2020, with an amino acid sequence with alignment (Fig. 1).

The SWISS-MODEL template library for evolutionarily related structures matching the target sequence is shown in Table 2. For details on the template search, were described in the Materials and Methods section above. Overall, 386 templates were found to match the target sequence. This list was filtered by a heuristic down to eight entries (Table 2). The eight highly identical templates are listed below with complete analysis of homology modeling parameters (Table 2). The GMQE value (0.99) was equal to every template (Table 2). The QSQE values ranged from 0.90 to 0.95 (Table 2). All the entries showed 100 significant identities (Table 2). The X-ray diffraction method for modeling studies with different resolutions ranging from 1.6 Å to 2.2 Å was considered (Table 2). Furthermore, all proteins were observed in the homo-dimer oligomeric state (Table 2). The prerequisite library annotated ligands were listed according to templates (Table 2).


Fig. 1. A predicted overview alignment for sequence similarity between the selected templates of the amino acid sequence.

*Table* 2

Summarizing the alignment parameters of highly identical templates to establish the relationship

| Name | Description | GMQE score | QSQE score | Identity | Method and resolution (Å) | Oligo state | Ligands |
|---|---|---|---|---|---|---|---|
| 6y2g.1.B | Replicase polyprotein 1ab | 0.99 | 0.95 | 100.00 | X-ray, 2.2 | homo-dimer | 1 x GLY, 2x O6K |
| 6m2n.1.A | SARS-CoV-2 3CL protease | 0.99 | 0.94 | 100.00 | X-ray, 2.2 | homo-dimer | 2 x 3WL |
| 6m2n.1.B | SARS-CoV-2 3CL protease | 0.99 | 0.94 | 100.00 | X-ray, 2.2 | homo-dimer | 2 x 3WL |
| 7buy.1.A | SARS-CoV-2 virus main protease | 0.99 | 0.94 | 100.00 | X-ray, 1.6 | homo-dimer | 2 x JRY |
| 6m2n.2.B | SARS-CoV-2 3CL protease | 0.99 | 0.93 | 100.00 | X-ray, 2.2 | homo-dimer | 2 x 3WL |

| | | | | | | | |
|---|---|---|---|---|---|---|---|
| 6wtk.1.A | 3C-like protease | 0.99 | 0.93 | 100.00 | X-ray, 2.0 | homo-dimer | 2 x UED |
| 6yz6.1.A | Main protease | 0.99 | 0.93 | 100.00 | X-ray, 1.7 | homo-dimer | 2 x ACE-LEU-LEU-AR7, 2 x IMD |
| 6wtj.1.B | 3C-like protease | 0.99 | 0.90 | 100.00 | X-ray, 1.9 | homo-dimer | 2 x K36 |

STRUCTURAL ASSESSMENT

The Ramachandran plot structural assessment was performed by MolProbity for further evaluation of model quality [6]. Numerical values of the MolProbity results are summarized with a resolution of 2.20 Å. Significantly, 1.08 MolProbity score, 97.67 % Ramachandran favored score and 35 out of 6493 bad angles were observed (Table 3).

*Table 3*

Protein conformational parameters for structural assessment by Ramchandran plot (MolProbity)

| **MolProbity score** | **Clash score** | **Ramachandran favored score** | **Rotamer outliers** | **C-Beta deviations** | **Bad bonds** | **Bad angles** |
|---|---|---|---|---|---|---|
| 1.08 | 0.32 | 97.67 % | 0.17 | 7 | 1/4780 | 35/6493 |

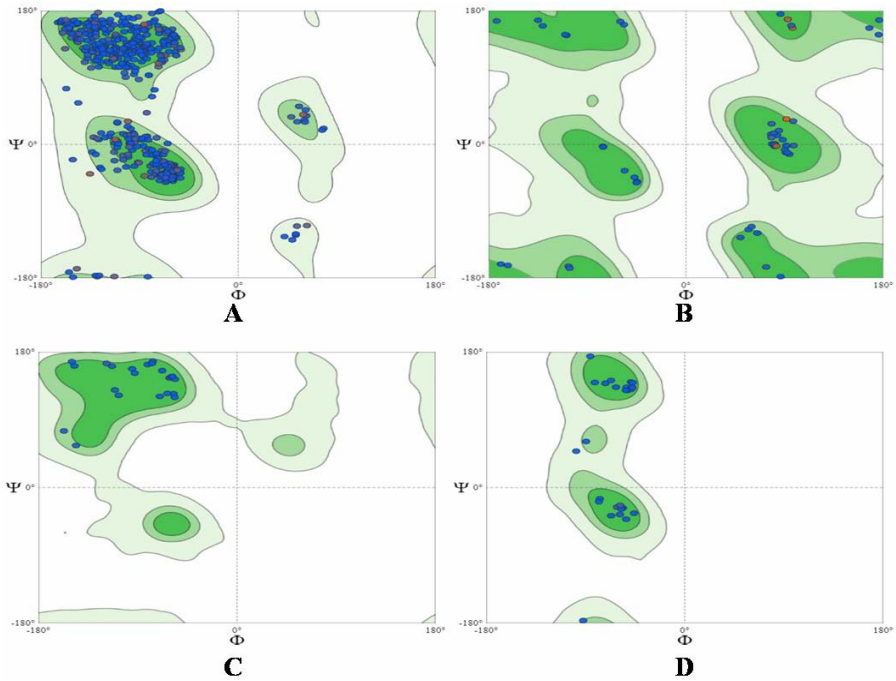


Fig. 2. Ramachandran plot obtained using MolProbity for overall protein (A) and for glycine (B), preproline (C), and proline (D) amino acids.

MAIN PROTEASE STRUCTURE

The individual predicted protein structure was obtained by clicking on a checkbox (Fig. 3A) and can be analyzed with different angle and conformational visualization models [4, 31]. Similarly, different template structure super positions were visualized and compared in 3D viewer (Fig. 3B). Templates selected according to target similarity coverage were found to be very similar and superimposed (Fig. 3B). However, some local dissimilarity was observed due to turns and loop regions (Fig. 3B).

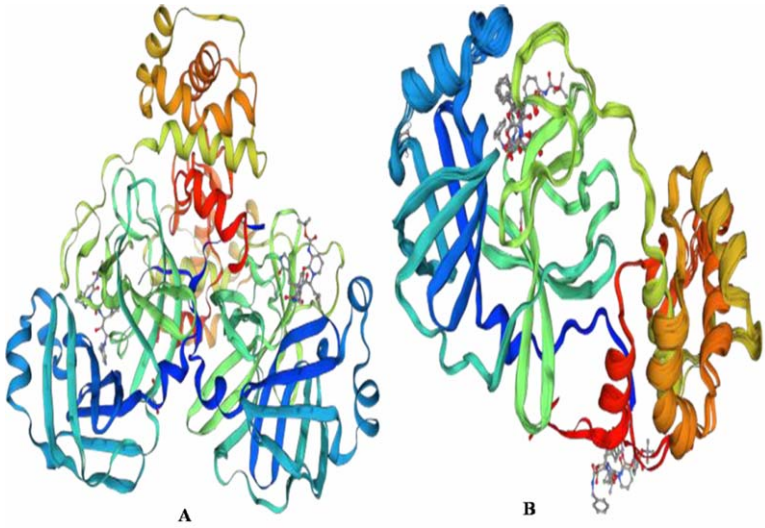


Fig. 3. SWISS-MODEL Structure (A) predicted the 3-dimensional structure of COVID-19 main protease and (B) superior structural alignment with different templates.

LOCAL QUALITY ESTIMATE AND COMPARISON

The local quality estimate was performed between the local similarity to the target and the number of residues. Two chains are shown in different colors in the target protein (Fig. 4). Here, both chains occurred abundantly between 0.8 and 1.0 predicted local similarity score with increasing residue number (Fig. 4A). The QMEAN score on the *y*-axis indicates the major geometrical aspects of protein structure, determining quality of the model (Fig. 4B). High comparison scores were obtained for high-resolution crystal structures [4, 31]. A comparison with the non-redundant set of PDB structures was observed between 0.5 and 1.0 normalized QMEAN score (Fig. 4B).

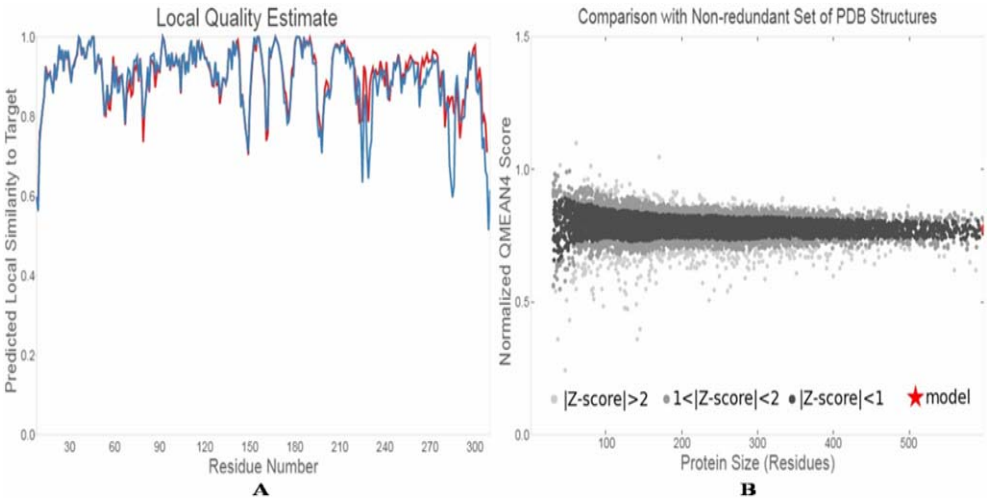


Fig. 4. The two criteria depicted for structural assessments are (A) local quality estimate and (B) comparison with non-redundant set of PDB structures.

SWISSDOCK

Binding modes are scored using their full fitness and clusters. The average value of the full fitness parameter of their elements was used to arrange clusters [8]. The molecular docking was performed with SwissDock based on the docking software EADock DSS, whose algorithm consists of the well-defined steps mentioned above in the Methods section [8]. Docking was performed with palmatine against the COVID–19 main protease complex. Evaluations of the binding modes are scored using their full fitness, clustered, thermodynamically significant $\Delta G$ value and energy minimization. Clusters are then ranked according to the significant $\Delta G$ of their elements from top to bottom (Table 3, Fig. 5A) [8]. Out of a total of 32 clusters, the most favorable eight clusters 0 with different cluster ranks, namely, 2, 1, 0, 3, 7, 6, 5 and 4, are illustrated with favorable matching parameters (Table 3, Fig. 5B). The hydrogen bond distance in combination with the assumed cluster was observed in the range of 1.725 Å to 2.464 Å (Fig. 5B). The most significant interactions observed with cluster rank 2, having $\Delta G$ = –8.281919 kcal·mol$^{-1}$, with energy minimization 55.8351 kJ·mol$^{-1}$, full fitness –1441.91 kJ·mol$^{-1}$, surfFul 227.317 and solvFull –1416.54, were observed (Table 3, Fig. 5C). The significant H-bond distance in the single cluster interaction ranged from 1.725 Å to 2.152 Å (Fig. 5B).

*Table 4*

Summarization of highly significant values of docking parameters calculated from Chimera [18, 29] S: indicates mutually exclusive states that can assign to docked compounds. V: viable compounds are interesting.

| S | Cluster | Cluster rank | Energy minimization (kJ·mol$^{-1}$) | Full fitness (kcal·mol$^{-1}$) | InterFull | IntraFull | $\Delta G$ (kcal·mol$^{-1}$) | SurfFull | SolvFull |
|---|---|---|---|---|---|---|---|---|---|
| V | 0 | 2 | 55.8351 | –1141.91 | –58.835 | 106.148 | –8.281919 | 227.317 | –1416.54 |
| V | 0 | 1 | 55.8351 | –1141.91 | –58.835 | 106.148 | –8.281919 | 227.317 | –1416.54 |
| V | 0 | 0 | 55.8351 | –1141.91 | –58.835 | 106.148 | –8.281919 | 227.317 | –1416.54 |
| V | 0 | 3 | 55.8372 | –1141.9077 | –58.7986 | 106.102 | –8.277759 | 227.319 | –1416.53 |
| V | 0 | 7 | 56.1598 | –1141.7334 | –58.8424 | 105.912 | –8.259844 | 227.327 | –1416.13 |
| V | 0 | 6 | 56.1598 | –1141.7334 | –58.8424 | 105.912 | –8.259844 | 227.327 | –1416.13 |
| V | 0 | 5 | 56.1598 | –1141.7334 | –58.8424 | 105.912 | –8.259844 | 227.327 | –1416.13 |
| V | 0 | 4 | 56.1598 | –1141.7334 | –58.8424 | 105.912 | –8.259844 | 227.327 | –1416.13 |

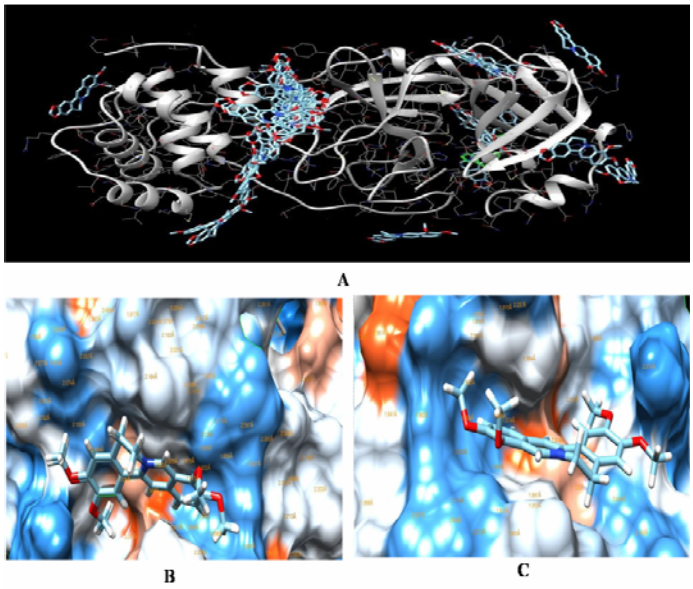


Fig. 5. The docking studies visualized in UCSF Chimera software were (A) the total available clusters are depicted upon binding with target molecule, (B) depicted interaction of ligand palmatine in vicinity with eight sites, (C) insight of most thermodynamically stable cluster rank 2 palmatine H-bond distance with target.

## COMPARATIVE DOCKING

For further validation of ligand molecule, comparative docking was performed with two different ligands namely, gingerol and berberine. The overall different docking parameters were calculated (Table 4). The significant $\Delta G$ value was observed for palmatine among the comparative ligand compounds (Table 4).

*Table 5*

Comparative docking analysis of palmatine with compound, namely gingerol and berberine, with the help of SwissDock and UNCF Chimera Tool.

| Sr No. | Inhibitor compound | Cluster rank | Energy minimization (kJ·mol$^{-1}$) | Full fitness (kcal·mol$^{-1}$) | Inter Full | Intra Full | Δ*G* (kcal·mol$^{-1}$) | Surf Full | SolvFull |
|---|---|---|---|---|---|---|---|---|---|
| 1 | Palmatine | 2 | 55.83 | –1141.91 | –58.83 | 106.14 | –8.28 | 227.31 | –1416.54 |
| 2 | Gingerol | 2 | –15 | –1215.00 | –46.32 | 8.06 | –7.42 | 227.31 | –1404.11 |
| 3 | Berberine | 2 | 48.86 | –1150.10 | –61.48 | 83.89 | –7.75 | 226.31 | –1398.82 |

## DISCUSSION

Palmatine is an alkaloid molecule with an active principle associated with a variety of biological activities of *Tinospora cordifolia* commonly named Guduchi [19, 21, 26, 30]. *T. cordifolia* belongs to the family *Menispermaceae*, which is a genetically diverse shrub naturally found in tropical regions of the Indian subcontinent [19, 21, 30]. From long back, it has been used in traditional medicine for the treatment of various disorders [19, 30]. *T. cordifolia* exhibits a variety of phytochemicals derived from plants, such as alkaloids, steroids, diterpenoid lactones, aliphatic, glycosides and other mixed compounds [30]. These compounds have been reported to have potential biological activities in different disease conditions, attracting applicability in clinical research [26]. It is anti-viral, anti-spasmodic, anti-microbial, anti-osteoporotic, anti-inflammatory, anti-arthritic, anti-allergic, and anti-diabetic conditions. Specifically, palmatine has been studied for use separately or in mixtures for the treatment of viral, jaundice, dysentery, hypertension, inflammation and liver-related diseases [26, 27]. Specifically, palmatine was reported to suppress dengue and yellow fever virus in a dose-dependent manner [13].

However, the mode of antiviral activity is not yet understood. Furthermore, the targeted molecules in the present study were analyzed with physico-chemical properties, revealing the functional acidic environment and hydrophobic nature of the protein (Table 1). The distance between different templates is proportional to the pairwise sequence similarity (Fig. 1). A highly identical score of predicted COVID-19 $M^{pro}$ is evolutionarily conserved. The protein predictions with individual target and template proteins showed reliable similarities (Fig. 3A, B). Typically, sequence variability affects the superposition structure by turns and loops (Fig. 3B). In other contexts, they are often involved in protein function; hence, they are of crucial importance in accurate modeling [9]. Structural assessment by local estimates for model quality based on the QMEAN scoring function is shown as a per-residue plot (Fig. 4A) and as a global score in relation to a set of high-resolution PDB structures (Z-score), as shown in Figure 4B. In the present study, the score is associated with each residue of the model (reported on the *x*-axis), reflecting the expected similarity to the native structure (*y*-axis). Residue scores < 0.6 are expected to be of low quality [12, 31]. Therefore, > 0.6 score for both the chains reveals high quality of protein

modelling (Fig. 4A). Furthermore, a higher QMEAN score comparison value indicates the quality of the model for experimental structures [12, 31], and similar results shown in Figure 4B provide reliable quality of the model.

The multifunctional COVID-19 main protease complex of SARS-CoV-2 was found to be involved in the replication and transcription of viral RNA responsible for the processing of polyprotein [14]. Additionally, host translational inhibition occurs by interacting with the host 40S ribosomal unit [14, 24, 33]. Similarly, different molecular functions have also been reported, such as helicase, protease and hydrolase [14, 24, 33]. Therefore, docking studies with $M^{pro}$ were carried out (Table 3, Fig. 5). The different docking parameters indicated reliable and promising ligand-protein interactions (Table 3, Fig. 5). Furthermore, comparative docking was performed with different ligands and $M^{pro}$ (Table 5). Among the three ligand-target interactions, palmatine interacts with a significant $-\Delta G$ value (Table 5). In conclusion, the multifunctionality of the main protease complex attracts potential drug targets. Therefore, an attempt was made to find a potent inhibitor against SARS-CoV-2 in the present pandemic. Further, *in vitro* studies are required for the confirmation of inhibitors. However, toxicity studies have reported that palmatine has an acute effect (135 mg/kg body weight) on the mouse model $LD_{50}$ [36, 42].

## CONCLUSIONS

Main protease complex was reported as a significant enzyme, mediating replication and transcription of the SARS-CoV-2. Therefore, it is attracting as potential drug target. Our *in silico* investigations suggest that alkaloid palmatine has potential inhibitory activity on $M^{pro}$. Appropriate molecular modeling was carried out with the available template(s). Docking studies reveal a potent inhibitory activity of palmatine against $M^{pro}$. Further, *in vitro* experimental investigations are required for the confirmation of our prediction.

*Acknowledgements*. Authors are thankful to Dr. Udhav Bhosale, Vice-Chancellor, S.R.T.M. University for his facilitation. Authors are thankful to research guide Dr. G.B. Zore, Director, CABIFF-MDCRL-COVID-19 Testing Laboratory, S.R.T.M. University for his encouragement and support. We are also, thankful to principal, Dr. P.A Chavan and colleagues, D.B. College, Bhokar. We are also thanks to Dr. Varsha Jadhav and Dear Research Lab mates, SLS, SRTM University.

## REFERENCES

1. AYITTEY, F.K., C. DZUVOR, M.K. AYITTEY, N.B. CHIWERO, A. HABIB, Updates on Wuhan 2019 novel coronavirus epidemic, *J. of Medical Virology*, 2020, **92**(4), 403–407.
2. BERTONI, M., F KIEFER, M. BIASINI, L. BORDOLI, T. SCHWEDE, Modeling protein quaternary structure of homo- and hetero-oligomers beyond binary interactions by homology, *Scientific Reports*, 2017, **7**(1), 1–15.
3. BOURNE, P.E., The protein data bank, in: *Protein Structure: Determination, Analysis, and Applications for Drug Discovery*, D.I. Chasman, ed., CRC Press, New York, 2003, pp. 389–406.

4. CAMACHO, C., G. COULOURIS, V. AVAGYAN, N. MA, J. PAPADOPOULOS, K. BEALER, T.L. MADDEN, BLAST+: architecture and applications, *BMC Bioinformatics*, 2009, **10**(1), 421–430.
5. CHEN, T., D. WU, H. CHEN, W. YAN, D. YANG, G. CHEN, K. MA, D. XU, H. YU, H. WANG, T. WANG, Clinical characteristics of 113 deceased patients with coronavirus disease 2019: retrospective study, *BMJ*, 2020, **26**, 368-m1091.
6. CHEN, V.B., W.B. ARENDALL, J.J. HEADD, D.A. KEEDY, R.M. IMMORMINO, G.J. KAPRAL, L.W. MURRAY, J.S. RICHARDSON, D.C. RICHARDSON, MolProbity: all-atom structure validation for macromolecular crystallography, *Acta Cryst. Section D: Biol Crys*., 2010, **66**(1), 12–21.
7. EFFERTH, T., F. HERRMANN, A. TAHRANI, M. WINK, Cytotoxic activity of secondary metabolites derived from *Artemisia annua* L. towards cancer cells in comparison to its designated active constituent artemisinin, *Phytomedicine,* 2011, **18**(11), 959–969.
8. GASTEIGER, E., C. HOOGLAND, A. GATTIKER, M.R. WILKINS, R.D. APPEL, A. BAIROCH, Protein identification and analysis tools on the ExPASy server, *The Proteomics Protocols Handbook*, Humana Press, 2005, pp. 571–607.
9. GROSDIDIER, A., V. ZOETE, O. MICHIELIN, EADock: docking of small molecules into protein active sites with a multiobjective evolutionary optimization, *Proteins: Structure, Function, and Bioinformatics*, 2007, **67**(4), 1010–1025.
10. GROSDIDIER, A., V. ZOETE, O. MICHIELIN, Fast docking using the CHARMM force field with EADock DSS, *J. of Comput. Chem.*, 2011b, **32**(10), 2149–2159.
11. GROSDIDIER, A., V. ZOETE, O. MICHIELIN, SwissDock, a protein-small molecule docking web service based on EADock DSS, *Nucleic Acids Research*, 2011a, **39**(suppl_2), W270–W277.
12. GUEX, N., M.C. PEITSCH, T. SCHWEDE, Automated comparative protein structure modeling with SWISS-MODEL and Swiss-PdbViewer: A historical perspective, *Electrophoresis*, 2009, **30**(S1), S162–S173.
13. JIA, F., G. ZOU, J. FAN, Z. YUAN, Identification of palmatine as an inhibitor of West Nile virus, *Archives of Virology*, 2010, **155**(8), 1325–1329.
14. JIN, Z., X. DU, Y. XU, Y. DENG, M. LIU, Y. ZHAO, B. ZHANG, X. LI, L. ZHANG, C. PENG, Y. DUAN, Structure of $M^{pro}$ from SARS-CoV-2 and discovery of its inhibitors, *Nature*, 2020, **582**, 289–293.
15. KHAZIR, J., B.A. MIR, S.A. MIR, D. COWAN, Natural products as lead compounds in drug discovery*, Journal of Asian Natural Products Research,* 2013, **15**, 764–788.
16. KIM, S., P.A. THIESSEN, E.E. BOLTON, J. CHEN, G. FU, A. GINDULYTE, L. HAN, J. HE, S. HE, B.A. SHOEMAKER, J. WANG, PubChem substance and compound databases, *Nucleic Acids Research,* 2016, **44**(D1), D1202–D1213.
17. LAI, C.C., T.P. SHIH, W.C. KO, H.J. TANG, P.R. HSUEH, Severe acute respiratory syndrome coronavirus 2 (SARS-CoV-2) and corona virus disease-2019 (COVID-19): the epidemic and the challenges, *I. J. of Antimicrobial Agents*, 2020, **55**(3), 105924.
18. MENG, E.C., PETTERSEN, E.F., COUCH, G.S., HUANG, C.C., T.E. FERRIN, Tools for integrated sequence-structure analysis with UCSF Chimera, *BMC Bioinformatics*, 2006, **7**(1), 339–348.
19. PARTHIPAN, M., V., ARAVINDHAN, A. RAJENDRAN, Medico-botanical study of Yercaud hills in the eastern Ghats of Tamil Nadu, India, *Ancient Science of Life,* 2011, **30**(4), 104–109.
20. PYRC, K., B. BERKHOUT, L. VAN DER HOEK, Identification of new human coronaviruses, *Expert Review of Anti-Infective Therapy*, 2007, **5**(2), 245–253.
21. RANA, V., K. THAKUR, R. SOOD, V. SHARMA, T.R. SHARMA, Genetic diversity analysis of *Tinospora cordifolia* germplasm collected from northwestern Himalayan region of India, *J. of Genetics*, 2012, **91**(1), 99–103.
22. REMMERT, M., A. BIEGERT, A. HAUSER, J. SÖDING, HHblits: lightning-fast iterative protein sequence searching by HMM-HMM alignment, *Nature Methods*, 2012, **9**(2), 173–175.

23. ROSE, P.W., B. BERAN, C. BI, W.F. BLUHM, D. DIMITROPOULOS, D.S. GOODSELL, A. PRLIĆ, M. QUESADA, G.B. QUINN, J.D. WESTBROOK, J. YOUNG, The RCSB protein data bank: redesigned web site and web services, *Nucleic Acids Research,* **39**(suppl_1), 2010, D392–D401.
24. ROTA, P.A., M.S. OBERSTE, S.S. MONROE, W.A. NIX, R. CAMPAGNOLI, J.P. ICENOGLE, S. PENARANDA, B. BANKAMP, K. MAHER, M.H. CHEN, S. TONG, Characterization of a novel coronavirus associated with severe acute respiratory syndrome, *Science,* 2003, **300**(5624), 1394–1399.
25. SABERI, A., A.A. GULYAEVA, J.L. BRUBACHER, P.A. NEWMARK, A.E., GORBALENYA, A planarian nidovirus expands the limits of RNA genome size, *PLoS Pathogens*, 2018, **14**(11), e1007314.
26. SAHA, S., S. GHOSH, *Tinospora cordifolia*: One plant, many roles, *Ancient Sci. of Life,* 2012, **31**(4), 151–159.
27. SHARMA, U., M. BALA, N. KUMAR, B. SINGH, R.K. MUNSHI, S. BHALERAO, Immunomodulatory active compounds from *Tinospora cordifolia*, *J. of Ethnopharmacology*, 2012, **141**(3), 918–926.
28. SHEREEN, M.A., S. KHAN, A. KAZMI, N. BASHIR, R. SIDDIQUE, COVID-19 infection: Origin, transmission, and characteristics of human corona viruses, *J. of Advanced Research,* 2020, **24**, 91–98.
29. STUDER, G., C. REMPFER, A.M. WATERHOUSE, R., GUMIENNY, J. HAAS, T. SCHWEDE, QMEAND is co-distance constraints applied on model quality estimation, *Bioinformatics,* 2020, **36**(6), 1765–1771.
30. UPADHYAY, A.K., K. KUMAR, A. KUMAR, H.S. MISHRA, *Tinospora cordifolia* (Willd.) Hook. f. and Thoms. (Guduchi) – validation of the Ayurvedic pharmacology through experimental and clinical studies, *I. J. of Ayurveda Resea.*, 2010, **1**(2), 112–121.
31. WATERHOUSE, A., M. BERTONI, S. BIENERT, G. STUDER, G. TAURIELLO, R. GUMIENNY, F.T, HEER, T.A.P. DE BEER, C. REMPFER, L. BORDOLI, R. LEPORE, SWISS-MODEL: homology modelling of protein structures and complexes, *Nucleic Acids Research*, 2018, **46**(W1), W296–W303.
32. WOO, P.C., Y. HUANG, S.K. LAU, K.Y. YUEN, Coronavirus genomics and bioinformatics analysis, *Viruses,* 2010, **2**(8), 1804–1820.
33. WU, F., S. ZHAO, B. YU, Y.M. CHEN, W. WANG, Z.G. SONG, Y. HU, Z.W. TAO, J.H. TIAN, Y.Y. PEI, M.L. YUAN, A new coronavirus associated with human respiratory disease in China, *Nature*, 2020, **579**(7798), 265–269.
34. ZHANG, L., D. LIN, X. SUN, U. CURTH, C. DROSTEN, L. SAUERHERING, S. BECKER, K. ROX, R. HILGENFELD, Crystal structure of SARS-CoV-2 main protease provides a basis for design of improved α-ketoamide inhibitors, *Science,* 2020, **368**(6489), 409–412.
35. ***http://www.ebi.ac.uk/chebi/searchId.do?chebiId=CHEBI:16096.
36. ***https://chem.nlm.nih.gov/chemidplus/sid/0003486677.
37. ***https://www.rcsb.org/structure/6LU7, Released**:** 2020-02-05.
38. ***https://web.expasy.org/protparam/
39. ***https://swissmodel.expasy.org/
40. ***https://www.ncbi.nlm.nih.gov/pccompound)
41. ***http://www.swissdock.ch/
42. ***https://chem.nlm.nih.gov/chemidplus/sid/0003486677
43. ***https://www.charmm.org//